ELSEVIER

Journal of Luminescence 86 (2000) 407–413

JOURNAL OF LUMINESCENCE

www.elsevier.com/locate/jlumin

# Laser-induced hole filling in reaction center of photosystem II

R. Dědic[a], M. Lovčinský[a], F. Vácha[b], J. Hála[a,*]

[a]*National Research Center of Photosynthesis and Global Climate Change, Department of Chemical Physics and Optics, Charles University, Ke Karlovu 3, CZ-12116 Praha 2, Czech Republic*

[b]*University of South Bohemia and Institute of Plant Molecular Biology, Academy of Sciences of the Czech Republic, Branišovská 31, CZ-37005 České Budějovice, Czech Republic*

**Abstract**

Laser-induced hole-filling of a primary hole (at $\lambda_{\mathrm{pri}}$) after burning of a secondary hole (at $\lambda_{\mathrm{sec}}$) was measured in $Q_y$ absorption spectra of the photosystem II reaction center at 4.2 K. The areas of the primary burnt holes were filled more for $\lambda_{\mathrm{pri}} > \lambda_{\mathrm{sec}}$ than for $\lambda_{\mathrm{pri}} < \lambda_{\mathrm{sec}}$. The observed laser-induced hole filling kinetics followed biexponential decays for $\lambda_{\mathrm{pri}} > \lambda_{\mathrm{sec}}$, while for $\lambda_{\mathrm{pri}} < \lambda_{\mathrm{sec}}$ they were only monoexponential. Two different laser-induced hole filling mechanisms were connected with two different decay parameters. The first laser-induced hole filling mechanism was interpreted as photoinduced relaxation of the protein matrix, while the second one was due to excited energy transfer in the reaction center of photosystem II. © 2000 Elsevier Science B.V. All rights reserved.

*Keywords:* Hole burning; Laser-induced hole filling; Exciton migration; Reaction center of photosystem II

## 1. Introduction

Photosystem II (PS II) is one of two main photosynthetic units in green plants and cyanobacteria. Photosystem II oxidizes water and provides electrons for reduction of carbon dioxide to organic substances. Photosystem II consists of antenna and reaction center (RC) complexes. The antenna complexes absorb visible light and transfer excitation to the primary electron donor within the RC, where the energy is trapped by a sequence of electron-transport reactions.

The PS II RC consists of the $D_1$ and $D_2$ proteins, the $\alpha$ and $\beta$ subunits of cytochrome $b_{559}$ and the product of the *psbI* gene. It was first isolated [1]. Since that time several PS II RC complex preparations containing well-defined numbers of chlorophylls *a* (Chl *a*), pheophytines *a* (Pheo *a*) and β-carotenes (β-Car) were prepared using other biochemical techniques, e.g. [2].

The molecular structure of the PS II RC is not well known, because it has not been up to now achieved sufficient resolution of X-ray diffraction and electron microscope studies. The understanding and interpretation of excited energy transfer and electron transport in PS II RC are therefore based mainly on homology of the $D_1$, $D_2$ proteins with the L and M proteins in the RC of purple bacteria, where the structural methods were successful, and on application of high-resolved spectroscopic studies of their functional properties. Fast (fs–ps) excited energy transfer and electron transport were widely studied directly by means of

---

[*] Corresponding author. Tel.: + 420-2-2191-1421; fax: + 420-2-2191-1249.

*E-mail address:* hala@karlov.mff.cuni.cz (J. Hála)

PII: S0022-2313(00)00183-6

time-resolved absorption and fluorescence spectroscopy as well as indirectly using hole-burning technique.

Spectral hole-burning investigations [3–5] consist of measuring of both resonant and off-resonant holes in low-temperature absorption, fluorescence and fluorescence excitation spectroscopy. Moreover, spontaneous and laser-induced hole filling (LIHF) studies provide additional information about hole burning and hole-filling mechanisms.

Spontaneous hole filling of cresyl violet in polyvinyl alcohol films was studied [6]. It was shown that the dominant mechanism for filling is an antihole reversion. Any global spectral diffusion did not play dominant role in hole filling. A positive correlation between the rates of burning and filling associated with the external two level systems (TLS) was found. The spontaneous hole-filling mechanism interpretation was based on the hypothesis that only a fraction of burned sites, on reversion to the ground state, yields sites with resonance frequencies that lie within the hole profile.

LIHF of primary hole after burning of a secondary hole at different wavelengths was measured and interpreted in several below mentioned papers. Shu and Small [7] concluded that the dominant LIHF mechanism in cresyl violet in polyvinylalcohol films is nonphotochemical (NPHB). They found that the LIHF mechanism in their NPHB system is the excitation of antihole site by the secondary burning. This LIHF mechanism involves electronic excitation of the antihole sites by means of their broad phonon side band. The dependence of the filling efficiency on the value of $\omega_B - \omega_S$ showed that the antihole sites retain at least a partial memory of their preburn configurations.

van den Berg and Völker [8] investigated LIHF of ionic dyes resorufin and cresyl violet in various glasses and polymers. The obtained results suggested that these ionic dye systems undergo intermolecular photochemical hole burning with high efficiency. The results indicated that the host polarity plays a key role in the photochemistry of these charged molecules. This explained the observed dependence on the wavelength. However, the area totally filled by LIHF in the absorption band was much larger than newly burned hole area.

Furusawa and Horie [9] interpreted LIHF phenomenon as the deactivation of dyes leading to structural relaxation around them. This model explained the decreased quantum efficiency of hole formation in photochemical hole burning (PHB) above 40 K. However, it also failed in explaining the observed dependence on the wavelength. Systematic LIHF measurements in PHB were performed in sulfonated tetraphenylporphin doped into polyvinylalcohol in Ref. [10]. The authors investigated mainly wavelength dependence of a hole-filling extent ($\gamma$). The hole-filling extent was defined as $\gamma = \lim_{E_B \to 0}[1 - \Delta D(E_B)/\Delta D(0)]/E_B$, where $\Delta D(E_B)$ is the primary hole depth after secondary burning using the burning energy $E_B$. The value of $\gamma$ was increasing with increasing spectral distance between primary and secondary burning wavelengths. Their quantitative LIHF interpretation was based on the existence of thermal excitation in the ground $S_0$ state. They found a potential function that describes the density of states of the doped dye to be a one-dimensional square well potential.

Few researchers have tried to interpret LIHF in systems with excited energy transfer (EET). Fearey et al. [11] discussed three possible LIHF mechanisms (thermal heating, site reversion and energy transfer) in dye-doped organic systems between individual impurity TLS via host TLS. However, this model was not able to explain the observed LIHF dependence on the wavelength. The role of EET in LIHF was further studied in fluorescence of core photosynthetic antennae in Refs. [12,13]. Two LIHF mechanisms were found to contribute to the observed results: One was interpreted as a light-induced structural relaxation (not involving spectral diffusion) which is effective for both $\lambda_{pri} \geq \lambda_{sec}$ and $\lambda_{pri} \leq \lambda_{sec}$ and which is independent on $\lambda_{sec} - \lambda_{pri}$. The authors in Refs. [12,13] suggested that next to structural relaxation an additional mechanism is present. This additional mechanism is effective only for $\lambda_{pri} \geq \lambda_{sec}$ and it is strongly dependent on the value of $\lambda_{pri} - \lambda_{sec}$. It originates from fast downward excited energy transfer within the CP 43 antenna. During the burning of the secondary hole at $\lambda_{sec}$ a part of absorbed energy is transferred towards chromophores absorbing at longer wavelengths. As this EET is not strictly directed, the energy is dissipated over certain spectral distribution of the final acceptors.

Kroh et al. [14] investigated LIHF in absorption of bacteriochlorophyll *d* monomers without any fast EET. They found that relative hole area decays monoexponentially with the secondary burning exposition. The decay (hole filling) coefficient slightly decreased with an increase in spectral distance between primary and secondary burning wavelengths $|\lambda_{\mathrm{pri}} - \lambda_{\mathrm{sec}}|$.

It is generally accepted that excited energy is very effectively transferred and finally trapped mainly in the PS II RC special pair even at low temperatures. The aim of this contribution is to present LIHF data obtained in PS II RC and to offer plausible interpretation of LIHF mechanism in the frame of EET within the PS II RC.

## 2. Materials

PS II RC containing 5 Chl *a* and 1 β-Car per 2 Pheo *a* were prepared from *Pisum sativum* by means of immobilized metal affinity chromatography according to Ref. [2]. The PS II RC samples were dissolved in 60% glycerol-buffer mixture to get the desired OD $\approx 1$ of PS II RC. The mixture was slowly frozen in a bath or gas-flow cryostat to produce transparent samples at low temperatures (4.2, 25 K).

## 3. Methods

Persistent hole-burning experiments were performed in absorption spectra of PS II RC containing 5 Chl *a* at 4.2 K. The absorption spectra were measured in single-channel mode by means of stabilized 200 W quartz tungsten halogen lamp together with double-grating monochromator (resolution 0.5 $\mathrm{cm}^{-1}$, sensitivity 0.001 OD). The scanning beam was focused together with the burning laser beam to the $\approx 1\ \mathrm{mm}^2$ area of the sample immersed in the bath cryostat. The absorption signal was detected by cooled photomultipliers along with a lock-in amplifier. The holes were burnt into $Q_y$ absorption band by a cw dye laser. (Spectra Physics 375B, equipped with 3-plate birefringent filter and thin etalon.) The spectral width of the laser was 0.3 $\mathrm{cm}^{-1}$. Zero fluence extrapolated value of zero phonon hole (ZPH) width was determined from the burning laser intensity and burning time fluence curves to remove a power broadening.

The effect of spontaneous filling of the primary hole was studied by measuring the ZPH at different delayed times $t_{\mathrm{d}}$ after measuring of the primary ZPH. The value of $t_{\mathrm{d}}$ ranged from $10^2$ to $10^4$ s.

Laser-induced hole-filling experiments were performed similarly as described in Refs. [12–14]. Primary hole was burnt by the cw dye laser ($P = 100\ \mathrm{mW\ cm}^{-2}$) tuned at the primary wavelength $\lambda_{\mathrm{pri}}$. Then the dye laser was tuned to the secondary burning wavelength $\lambda_{\mathrm{sec}} \neq \lambda_{\mathrm{pri}}$ and the whole procedure of hole burning using a laser power ($P = 50\ \mathrm{mW\ cm}^{-1}$) and increasing burning time ($0 \leq t \leq 3000$ s) was repeated. A correction of the different sample optical density at different burning wavelengths was taken into account. Relative hole-filled area $[A_0 - A]/A$ increased with increasing of the secondary burning exposition $Pt$, where $A_0$ is the area of the primary burnt hole before the burning of the secondary hole ($t = 0$). The mathematical description of the function $A = A(P, t, \lambda_{\mathrm{pri}}, \lambda_{\mathrm{sec}})$ was systematically studied for various $\lambda_{\mathrm{pri}}$ and $\lambda_{\mathrm{sec}}$.

## 4. Results

Fig. 1 shows typical low-temperature $Q_y$ absorption and (0–0) fluorescence spectra of the PS II RC. The relatively high absorption band at 670 nm is mainly due to scattered light in our samples and not due to disrupted chlorophylls. The wavelengths of $\lambda_{\mathrm{pri}}$ and $\lambda_{\mathrm{sec}}$ ranged between 674 and 686 nm. Typical dependence of the ZPH width $\delta_{\mathrm{ZPH}} = \delta_0 + a(Pt)^{\mathrm{b}}$ measured in the primary burning ($\lambda_{\mathrm{pri}} = 680.0$ nm) is shown in Fig. 2. $P$ is the burning power, $t$ is the burning time. This fluence dependence was the same whether the hole is burnt as primary or as secondary one. The obtained values ranged $6 \leq \delta_0 \leq 7\ \mathrm{cm}^{-1}$, while $b \approx 0.25$ for $\lambda_{\mathrm{pri}} = 680.0$ and 682.6 nm. Fig. 3 documents the dependence of the ZPH area $A$ on $Pt$. The burnt hole area dependence is shown for data obtained both from hole area integration and from hole fit

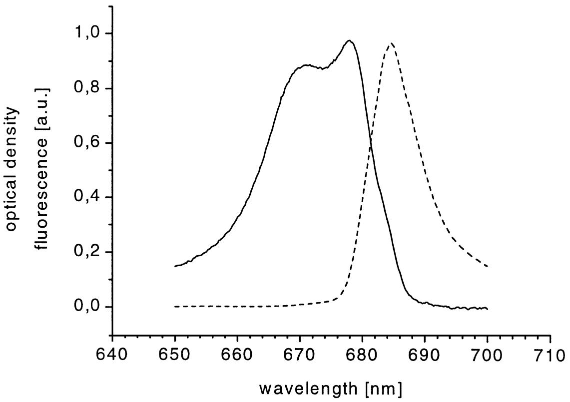

Fig. 1. Low-temperature $Q_y$ absorption (full line) and (0–0) fluorescence (dashed line) spectra of reaction center of photosystem II containing 5 Chl *a*, 2 Pheo *a* and 1 β-Car.

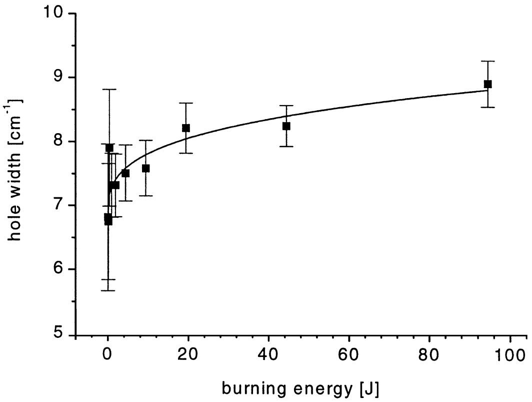

Fig. 2. Typical fluence dependence $\delta_{\mathrm{ZPH}} = \delta_0 + a(Pt)^{\mathrm{b}}$ measured in the primary burnt hole at 680.0 nm.

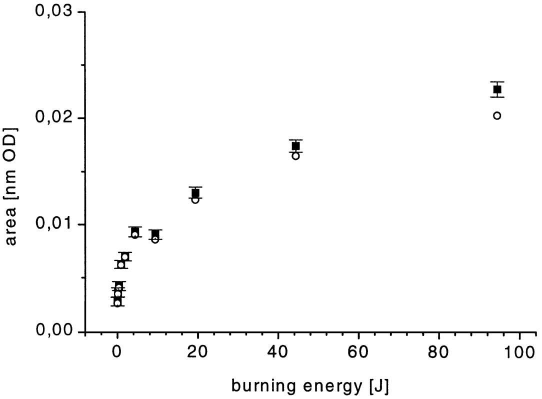

Fig. 3. Typical dependence of the burnt ZPH area $A = A(Pt)$ measured in the primary burnt hole at $\lambda_{\mathrm{pri}} = 680.0$ nm. Circles represent the integrated hole area, squares are values calculated from Gaussian hole profile fits.

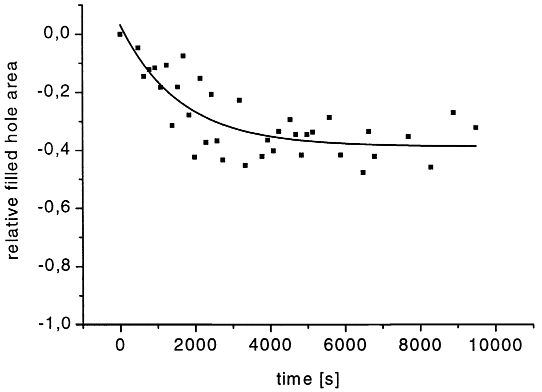

Fig. 4. Spontaneous hole filling of the primary burnt hole at 680.0 nm. The ZPH area value $A = A_0 \exp(-t_{\mathrm{d}}/\tau_{\mathrm{S}})$, against the time $t_{\mathrm{d}}$ after the primary burning.

calculation. From these dependencies we have chosen the burning dose $Pt = 60$ J to monitor hole filing of the semisaturated ZPH.

It was shown that spontaneous hole filling of the primary burnt holes does not influence the $\delta_{\mathrm{ZPH}}$. The value of $\delta_{\mathrm{ZPH}} = 9.0 \pm 0.4\ \mathrm{cm}^{-1}$ was the same even after $10^4$ s (data not shown). On the other hand, the value of $A$ was decreasing with time $t_{\mathrm{d}}$ of the second measuring after primary hole burning. Fig. 4 shows a typical dependence of hole area burnt at 680.0 nm against the time. The spontaneous hole-filling data were fitted by monoexponential decay $A = A_0 \exp(-t_{\mathrm{d}}/\tau_{\mathrm{S}})$, where $\tau_{\mathrm{S}} = 1600$ s. This fit was latter used for subtraction of spontaneous hole filling from all LIHF data.

Typical laser-induced hole-filling spectra are documented in Fig. 5. Absorption spectrum of PS II RC after primary burning is shown above. A deep burnt ZPH at $\lambda_{\mathrm{pri}}$ was filled during the secondary burning. After the secondary burning using the same exposition the LIHF is less efficient for $\lambda_{\mathrm{pri}} < \lambda_{\mathrm{sec}}$ (middle) in comparison with that for $\lambda_{\mathrm{pri}} > \lambda_{\mathrm{sec}}$ (bottom). Moreover, we found that LIHF efficiency increases (66–100%) with an increase in value of $\lambda_{\mathrm{pri}} - \lambda_{\mathrm{sec}}$ for all $\lambda_{\mathrm{pri}} > \lambda_{\mathrm{sec}}$. On the other hand, the LIHF efficiency is practically

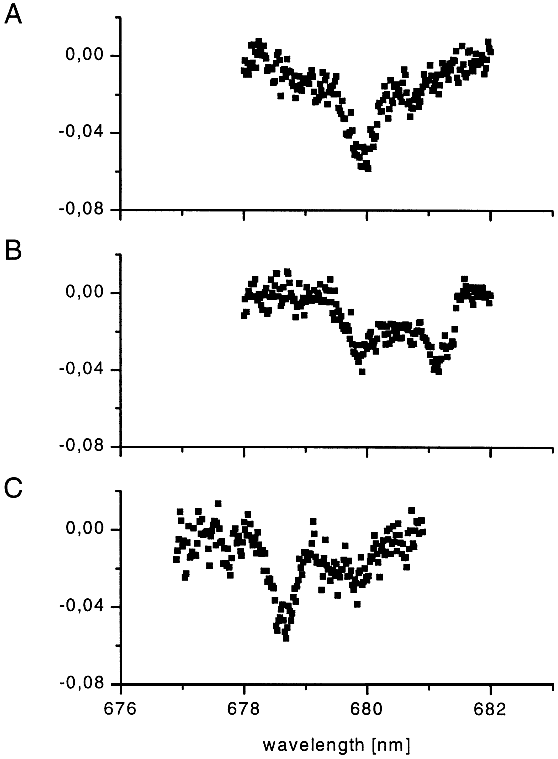

Fig. 5. Typical laser-induced hole-filling spectra. Absorption spectrum of PS II RC with a deep burnt ZPH at $\lambda_{\mathrm{pri}} = 680.0$ nm after primary burning is shown above. After the secondary burning using the same exposition the LIHF is less efficient for $\lambda_{\mathrm{sec}} = 681.4$ nm (middle) in comparison with that for $\lambda_{\mathrm{sec}} = 678.6$ nm (bottom).

constant (45%) for $\lambda_{\mathrm{pri}} < \lambda_{\mathrm{sec}}$. The LIHF decays can be fitted by monoexponential curves following the expression $A(Pt) = A_0 + p\exp[-Pt/\tau_{\mathrm{R}}]$ for all $\lambda_{\mathrm{pri}} < \lambda_{\mathrm{sec}}$ (see Fig. 6). The parameter $\tau_{\mathrm{R}}$ values were on the order of 10 J for all LIHF performed outside the pseudo-phonon wing. On the other hand, LIHF decays cannot be fitted by monoexponential function for $\lambda_{\mathrm{pri}} > \lambda_{\mathrm{sec}}$. They can be fitted successfully by biexponential curves following the expression $A(Pt) = A_0 + p\exp[-Pt/\tau_{\mathrm{R}}] + q\exp[-Pt/\tau_{\mathrm{E}}]$ (see Fig. 7). The coefficients $\tau_{\mathrm{R}}$ were comparable to previous case, while coefficients $\tau_{\mathrm{E}}$ ranged about 1.2 J. The value of $\tau_{\mathrm{R}}$ decreases (from 40 to 10 J) with an increase in spectral distance of primary and secondary burning wavelengths $|\lambda_{\mathrm{pri}} - \lambda_{\mathrm{sec}}|$ for both above mentioned cases. The values of LIHF parameters $\tau_{\mathrm{R}}$ and $\tau_{\mathrm{E}}$ are plotted against the spectral distance of primary and secondary burning wavelengths in Fig. 8.

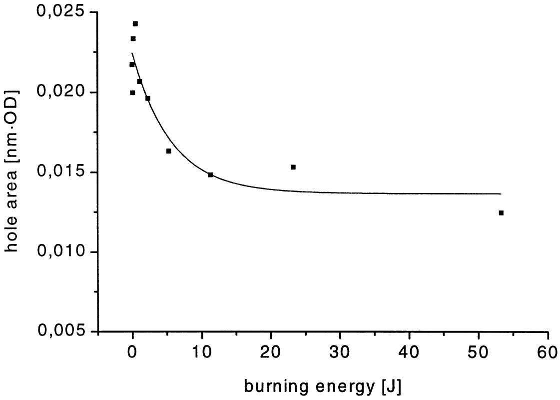

Fig. 6. Monoexponential laser-induced hole-filling decay of the primary burnt ZPH area for $\lambda_{\mathrm{pri}} < \lambda_{\mathrm{sec}}$, $\lambda_{\mathrm{pri}} = 680.0$ nm, $\lambda_{\mathrm{sec}} = 681.4$ nm.

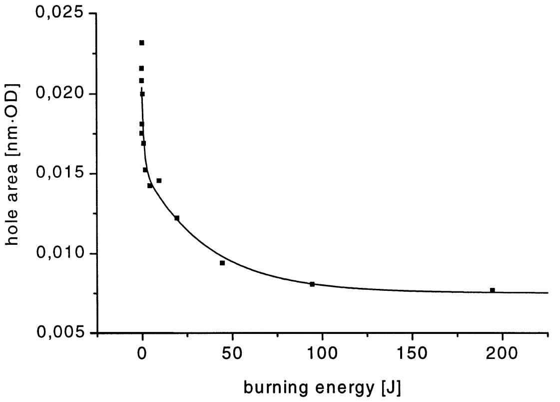

Fig. 7. Biexponential laser-induced hole filling decay of the primary burnt ZPH area for $\lambda_{\mathrm{pri}} > \lambda_{\mathrm{sec}}$, $\lambda_{\mathrm{pri}} = 680.0$ nm, $\lambda_{\mathrm{sec}} = 678.6$ nm.

## 5. Discussion

LIHF was found to be more pronounced for $\lambda_{\mathrm{pri}} > \lambda_{\mathrm{sec}}$ than that for $\lambda_{\mathrm{pri}} < \lambda_{\mathrm{sec}}$. The same qualitative trends in the filling hole depths were obtained in Refs. [9,10,12–14]. The filled hole area reached 45% for all $\lambda_{\mathrm{pri}} < \lambda_{\mathrm{sec}}$ independent of the

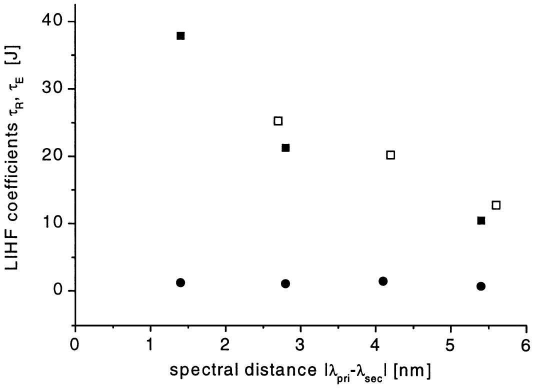

Fig. 8. The values of LIHF parameters $\tau_R$ and $\tau_E$ plotted against the spectral distance of primary and secondary burning wavelengths $|\lambda_{pri} - \lambda_{sec}|$. Circles represent $\tau_E$, full and open squares denote $\tau_R$ for $\lambda_{pri} > \lambda_{sec}$ and $\lambda_{pri} < \lambda_{sec}$, respectively.

value of $\tau_R$. This value corresponds to that part of the primary burnt sites which were recovered during LIHF. From this fact it is evident that remaining 55% of the sites changed their protein environment during primary burning so dramatically, that they were not able to recover during secondary burning at $\lambda_{pri} < \lambda_{sec}$. On the other hand, the filled hole area increased (from 66 to 100%) with increasing spectral distance of primary and secondary burning wavelengths $\lambda_{sec} - \lambda_{pri}$. Such efficient LIHF can be either due to absorption and vibrational relaxation of higher energy of the secondary burning, or due to downward EET. It is impossible to decide the prevailing mechanism from studies of the filled hole area only.

Additional information can be obtained from LIHF kinetics (fluences). These LIHF kinetics reflect a correlation between primary and secondary burnt sites. The LIHF kinetics are connected with LIHF mechanisms. The LIHF kinetics for $\lambda_{pri} < \lambda_{sec}$ follow monoexponential decay. The monoexponential decay corresponds to single LIHF mechanism. The same monoexponential behavior was found in bacteriochlorophyll *d* monomers [14]. On the other hand, the LIHF decay cannot be fitted by monoexponential function for $\lambda_{pri} > \lambda_{sec}$. For this case at least biexponential decay must be invoked. The LIHF coefficients $\tau_R$ are in a very good agreement with those found in the monoexponential decay. The agreement of $\tau_R$ values for both $\lambda_{pri} < \lambda_{sec}$ and $\lambda_{pri} > \lambda_{sec}$ together with their identical dependencies on the spectral distance of primary and secondary burning wavelengths $|\lambda_{pri} - \lambda_{sec}|$ implies the same LIHF mechanism (see Fig. 8). This LIHF mechanism is believed to be photoinduced relaxation of the protein matrix. This photoinduced relaxation occurs for all $\lambda_{sec}$ in the $Q_y$ absorption band. The photoinduced relaxation could originate from conformational and vibrational changes of the protein matrix followed by recovery of the primary burnt sites. LIHF technique is not able to determine details of this mechanism. As the second LIHF coefficient $\tau_E$ was found only for $\lambda_{pri} > \lambda_{sec}$ and as it is independent on $\lambda_{pri} - \lambda_{sec}$ in the spectral region studied, we conclude that $\tau_E$ represents another (second) LIHF mechanism. The more effective ($\approx 1$ J) LIHF decay has not been observed in similar system without excited energy transfer in Ref. [14]. For these reasons we interpret the LIHF mechanism in PS II RC as being due to backward photoconversion of the antihole sites. These antihole sites are excited indirectly by means of fast EET from the sites absorbing at $\lambda_{sec}$. Our LIHF results obtained in PS II RC containing 5 Chl *a* are in good agreement with LIHF trends observed in the core antenna of PS II [12,13].

The $Q_y$ region of PS II RC absorption spectrum can be deconvoluted into three main bands at 670, 680, and 684 nm [15,16]. The absorption at 670 nm is due to two chlorophyll molecules located at the peripheral histidins His118 and the $D_1$ and $D_2$ proteins and which transfer energy to the primary donor. The main band at 680 nm is due to the absorption of the primary electron donor P680. The absorption at 684 nm is still a matter of debate but it was recently concluded that this absorption is due to the low-energy exciton band of the primary donor P680 which can act as an energy trap. This trap is not involved in the energy transfer [4,17]. Therefore, for $\lambda_{pri} < \lambda_{sec}$ there is no energy transfer since all the energy is trapped by the 684 nm chlorophyll population. If the secondary hole is burnt at $\lambda_{pri} > \lambda_{sec}$ a part of the energy may be transferred to the primary donor by the peripheral chlorophyll molecules which absorb at 670 nm. The absence of the energy transfer LIHF mechanism for

$\lambda_{\mathrm{pri}} < \lambda_{\mathrm{sec}}$ supports the idea that the 684 nm chlorophyll pool cannot act in the energy transfer.

## 6. Conclusions

The phenomenon of laser-induced hole filling of a primary hole after burning of a secondary hole in absorption spectra at different wavelengths was studied in PS II RC. Two different LIHF mechanisms were found in PS II RC. The first was interpreted as photoinduced relaxation of the protein matrix, while the second one is due to excited energy transfer.

## Acknowledgements

This work was supported by following projects: MŠMT 97113 and 96085, VZ J13/98:11320001, GAČR 202/97/P097, 204/98/P121 and GAUK 175/1999/B.

## References

[1] O. Namba, K. Satoh, Proc. Natl. Acad. Sci. USA 84 (1987) 109.
[2] F. Vácha, D.M. Joseph, J.R. Durrant, A. Telfer, D.R. Klug, G. Porter, J. Barber, Proc. Natl. Acad. Sci. USA 92 (1995) 2929.
[3] D. Tang, R. Jankowiak, M. Seibert, C.F. Yocum, G.J. Small, J. Phys. Chem. 94 (1990) 6519.
[4] M.L. Groot, J.P. Dekker, R. van Grondelle, F.T.H. den Hartog, S. Völker, J. Phys. Chem. 100 (1996) 11 488.
[5] F.T.H. den Hartog, F. Vacha, A.J. Lock, J. Barber, J.P. Dekker, S. Völker, J. Phys. Chem. B 102 (1998) 9174.
[6] L. Shu, G.J. Small, J. Opt. Soc. Am. B 9 (1992) 733.
[7] L. Shu, G.J. Small, J. Opt. Soc. Am. B 9 (1992) 738.
[8] R. van den Berg, S. Völker, Chem. Phys. 128 (1988) 257.
[9] A. Furusawa, K. Horie, J. Chem. Phys. 94 (1991) 80.
[10] N. Murase, K. Horie, Chem. Phys 183 (1994) 135.
[11] B.L. Fearey, T.P. Carter, G.J. Small, Chem. Phys. 101 (1986) 279.
[12] M. Vácha, F. Adamec, M. Ambrož, J. Pšenčík, J. Hála, J. Molecular Struct. 294 (1993) 131.
[13] M. Vácha, J. Pšenčík, F. Adamec, M. Ambrož, J. Dian, L. Nedbal, J. Hála, J. Lumin. 60–61 (1994) 523.
[14] P. Kroh, J. Pšenčík, T. Polívka, D. Engst, J. Hála, Mol. Crystallogr. Liq. Cryst. 291 (1996) 201.
[15] L. Konermann, I. Yruela, A. Holtzwarth, Biochemistry 36 (1997) 7498.
[16] C. Eijckelhoff, F. Vácha, R. van Grondelle, J.P. Dekker, J. Barber, Biochim. Biophys. Acta 1318 (1997) 226.
[17] F.T.H. den Hartog, J.P. Dekker, R. van Grondelle, S. Völker, J. Phys. Chem. B 102 (1998) 11 007.